THE PROTEIN SOCIETY

5′-*N*-ethylcarboxamidoadenosine is not a paralog-specific Hsp90 inhibitor

Shanshan Liu and Timothy O. Street*

Department of Biochemistry, Brandeis University, Waltham, MA 02454

Received 10 August 2016; Accepted 21 September 2016
DOI: 10.1002/pro.3049
Published online 26 September 2016 proteinscience.org

Abstract: The molecular chaperone Hsp90 facilitates the folding and modulates activation of diverse substrate proteins. Unlike other heat shock proteins such as Hsp60 and Hsp70, Hsp90 plays critical regulatory roles by maintaining active states of kinases, many of which are overactive in cancer cells. Four Hsp90 paralogs are expressed in eukaryotic cells: Hsp90α/β (in the cytosol), Grp94 (in the endoplasmic reticulum), Trap1 (in mitochondria). Although numerous Hsp90 inhibitors are being tested in cancer clinical trials, little is known about why different Hsp90 inhibitors show specificity among Hsp90 paralogs. The paralog specificity of Hsp90 inhibitors is likely fundamental to inhibitor efficacy and side effects. In hopes of gaining insight into this issue we examined NECA (5′-*N*-ethylcarboxamidoadenosine), which has been claimed to be an example of a highly specific ligand that binds to one paralog, Grp94, but not cytosolic Hsp90. To our surprise we find that NECA inhibits many different Hsp90 proteins (Grp94, Hsp90α, Trap1, yeast Hsp82, bacterial HtpG). NMR experiments demonstrate that NECA can bind to the N-terminal domains of Grp94 and Hsp82. We use ATPase competition experiments to quantify the inhibitory power of NECA for different Hsp90 proteins. This scale: Hsp82 > Hsp90α > HtpG ≈ Grp94 > Trap1, ranks Grp94 as less sensitive to NECA inhibition. Because NECA is primarily used as an adenosine receptor agonist, our results also suggest that cell biological experiments utilizing NECA may have confounding effects from cytosolic Hsp90 inhibition.

Keywords: chaperone; Hsp90; Grp94; NECA; inhibitor

Introduction

The highly conserved family of Hsp90 molecular chaperones plays a critical role in cellular homeostasis. Similar to other well-studied heat shock proteins such as Hsp60 and Hsp70, Hsp90 function requires ATP binding and hydrolysis.[1] However, in contrast to these other classic chaperone systems, Hsp90 plays a crucial role in normal cellular functioning by maintaining the activities of numerous signaling proteins, such as kinases.[2] The strong dependence of oncogenic kinases on the function of Hsp90 has spurred numerous ongoing clinical trials testing Hsp90 inhibitors as potential cancer therapies.[3]

Additional Supporting Information may be found in the online version of this article.

Disclosure: The authors have no conflict of interest to declare.

*Correspondence to: T. O. Street; 415 South St., Brandeis University, Waltham, MA 02454. E-mail: tstreet@brandeis.edu

Four distinct Hsp90 proteins are expressed in metazoans: Hsp90β (constitutively expressed in the cytosol); Hsp90α (heat-shock inducible in the cytosol); Trap1 (mitochondria specific); Grp94 (endoplasmic reticulum specific). These Hsp90 "paralogs" share a common domain structure (N-terminal domain, NTD; middle domain, MD; C-terminal domain, CTD) and a common set of ATP-driven conformational changes.[4] All Hsp90 paralogs require ATP binding and hydrolysis to perform their biological functions of maintaining the folding and activity of their target proteins.[1,5,6] Chemical inhibitors that block ATP binding at the Hsp90 NTD cause rapid degradation of these "client protein" targets.

Hsp90 paralogs have high sequence and structural homology in the ATP binding site, and as a consequence none of the commonly used chemical inhibitors bind specifically to just one paralog. Therefore, the individual effects of inhibiting Hsp90α,

Hsp90β, Trap1, and Grp94 are unavoidably intermixed. A paralog-specific inhibitor would be valuable for dissecting the individual biological roles of Hsp90 paralogs. This goal has brought recent attention to the possibility of developing a Grp94-specific inhibitor.[7]

Grp94 is arguably the least well-understood Hsp90 family member. The relatively short list of identified Grp94-dependent client proteins[8] is confounded with potential overlap with cytosolic Hsp90 clients. A prominent example is HER2, with differing reports arguing that the inhibitor-driven degradation of HER2 is a result of either Grp94 or cytosolic Hsp90.[9–13] A paralog-specific inhibitor could address this important question.

The plausibility of developing a Grp94-specific inhibitor has been motivated by a report that a small-molecule agonist of the adenosine receptor, NECA (5′-*N*-ethylcarboxamidoadenosine), could bind to Grp94 but not cytosolic Hsp90.[14] However, the cytosolic Hsp90 used in that study showed minimal binding of ATP and no ATPase measurements were performed to test whether the protein was active. A subsequent crystallographic study identified a unique binding mode of NECA to the Grp94 NTD, which led to a structural model to explain the presumed NECA specificity.[15]

Building on this structural model, large-scale efforts are now underway to develop Grp94-specific inhibitors,[16,17] in part motivated by the idea that NECA is a proof in principle that a totally paralog-specific ligand could be achieved. Because of its assumed specificity, NECA has been used in cell biology experiments attempting to separate the effects of Grp94 inhibition from cytosolic Hsp90 inhibition.[18] None of the previous studies reproduced the initial measurement that suggested NECA specificity towards Grp94.

In performing control experiments we discovered that NECA inhibits a wide variety of Hsp90 proteins. In this paper, we show that NECA is not a paralog-specific inhibitor.

Results

Reverse-phase chromatography demonstrates that our NECA stock suffers no contamination by ATP, ADP, AMP [Fig. 1(B)]. In contrast, our ADP stocks contain trace contamination of ATP and AMP [Fig. 1(B), inset].

To confirm that NECA binds to the NTD of Grp94, we utilized NMR to assign the Grp94 NTD in both the apo and NECA-bound states (151/228 residues, 66% and 186/228 residues, 82%, respectively). The 43 residues that could be assigned in the NECA-bound state but not in the apo state cluster to a region containing previously established flexible regions of the N-terminal domain (Supporting Information Fig. S1), suggesting that NECA reduces conformational heterogeneity.

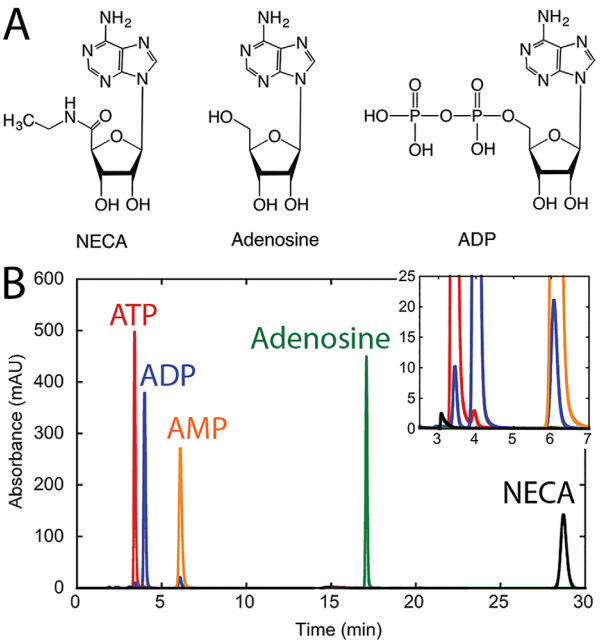

Figure 1. Structure and purity of NECA and adenosine nucleotides. **(A)** Chemical structures of NECA, adenosine, and ADP. **(B)** Reverse-phase chromatographic analysis of ligands used in this study. NECA has a unique retention time and no measurable contamination of ATP, ADP, AMP, or adenosine. The inset shows trace contamination of AMP and ATP in ADP stock solutions.

The NMR results show that NECA interacts in a unique manner, as expected from a previous crystal structure of NECA bound to the Grp94 NTD.[15] Specifically, we observe a large number of chemical shift changes located at a NECA binding site observed crystallographically (Supporting Information Fig. S1). Some of the chemical shift changes we observe are unique to NECA relative to other nucleotides. For example, Figure 2(B) shows an HSQC region in which certain peaks are observed in the presence of NECA, but not in the presence of ADP. Figure 2(C) illustrates that these NECA-specific peaks correspond to residues in NECA-specific conformations observed crystallographically. We conclude that our NMR measurements are consistent with the previously described crystal structure of NECA bound to the NTD.

Similar NMR measurements on the NTD of Hsp82 demonstrate that NECA can bind to a non-Grp94 paralog (Fig. 3). Since this result was not initially anticipated we sought further methods to test whether NECA is behaving as expected for a nucleotide-competitive inhibitor. To determine whether NECA can prevent nucleotide-driven closure of Hsp82, we utilized small angle X-ray scattering (SAXS). Hsp82 undergoes a large open/closed conformational change in the presence of nonhydrolyzable

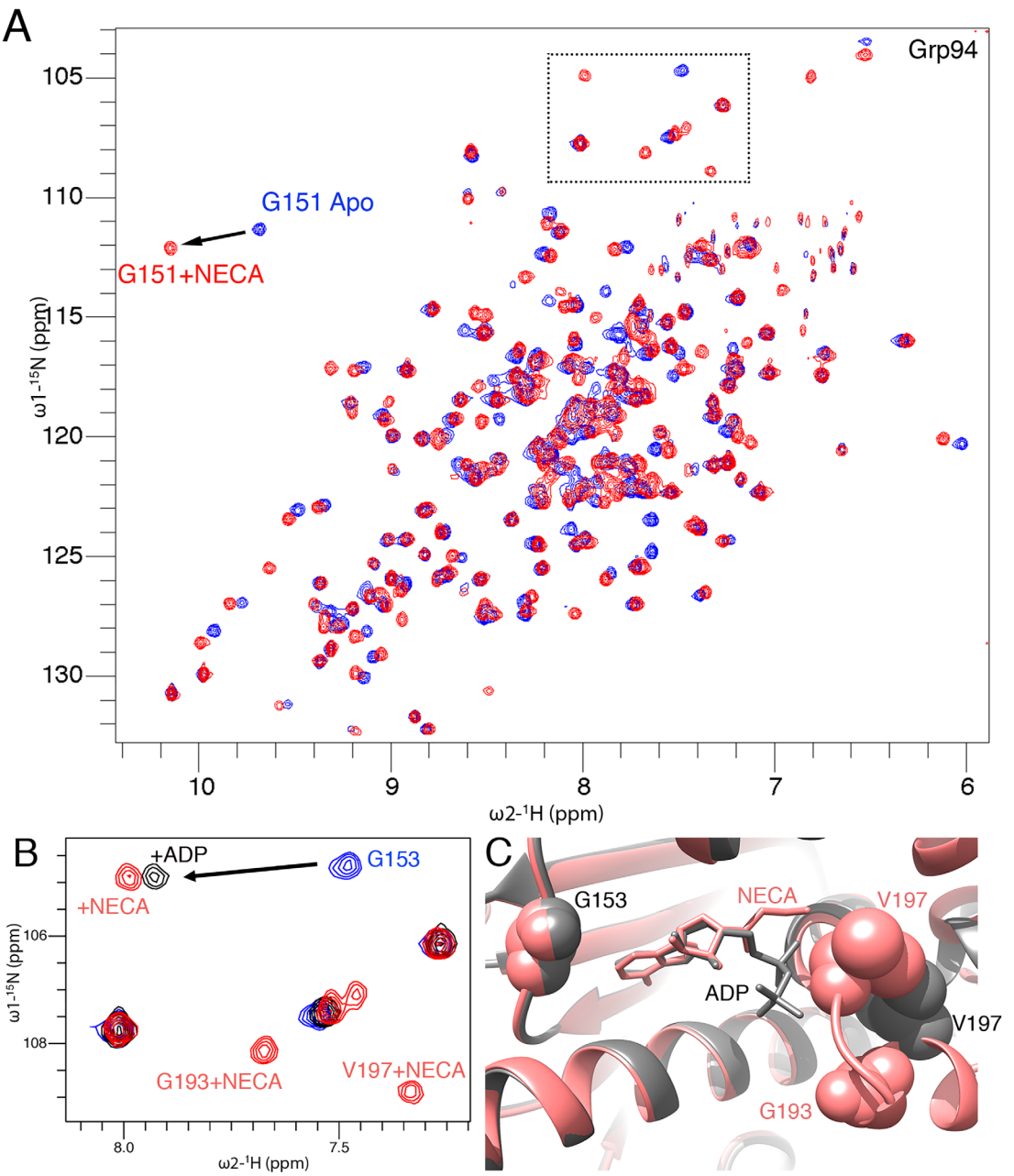

Figure 2. NECA has a unique mode of binding to the Grp94 NTD. (**A**) Numerous chemical shift perturbations of the NTD are observed from NECA binding. Buffer conditions: 25 m*M* KH_2PO_4 pH 7.0, 50 m*M* KCl, 2 m*M* BME, 293 K. **(B)** Example of residues with NECA-specific chemical shift changes. **(C)** Grp94 NTD structures bound to ADP (dark gray, 1TC6) and NECA (red, 1U2O) are consistent with the unique structural consequences of NECA binding observed by NMR.

ATP analogs such as AMPPNP, a change that is readily detectable by SAXS.[19–21] Closure is evident from a general reduction in interatomic scattering distances within the dimer. Supporting Information Figure S2 illustrates that NECA prevents AMPPNP-driven closure of Hsp82, as expected for an inhibitor.

Quantifying NECA inhibitory power for Hsp90 family members

To gauge the level of NECA specificity for a wide spectrum of Hsp90 family members we tested the power of NECA to inhibit the ATPase of Grp94, Hsp82, Hsp90α, HtpG, and Trap1. We employed traditional competitive inhibition experiments in which Hsp90 ATPase activity was measured by an enzyme linked assay and increasing NECA concentrations were used to inhibit Hsp90. These experiments were performed at variable concentrations of ATP (yellow, red, green, and blue symbols indicate low to high ATP concentrations in Fig. 4). As expected, ATPase activity of Grp94 is sharply inhibited by NECA, and as ATP increases more NECA is required to achieve full inhibition [Fig. 4(A)]. The solid lines in Figure 4(A,C) show that this data can be fit well with a

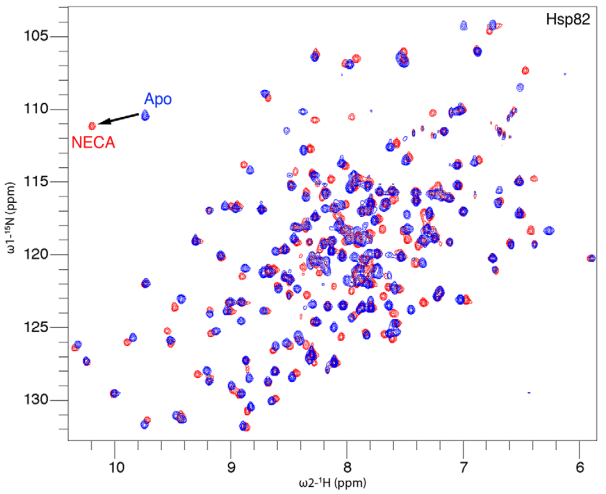

Figure 3. NECA binds to the Hsp82 NTD. Numerous chemical shift perturbations of the Hsp82 NTD are observed from NECA binding. Buffer conditions: 25 m*M* KH_2PO_4 pH 7.0, 50 m*M* KCl, 293 K.

simple competitive inhibition model [Eq. (2)(3) in "Methods"]. We find that the same concentration range of NECA results in a more pronounced inhibition of Hsp82 [Fig. 4(C)] indicating that Hsp82 is more sensitive than Grp94 to NECA inhibition. Similar competitive inhibition experiments were performed on Hsp90α, HtpG, and Trap1 (Supporting Information Fig. S3).

A simple competitive inhibition model predicts a linear relationship between the NECA concentration at which activity is reduced by half, $[NECA]_{IC50}$, and the ATP concentration [Eq. (4) in "Methods"]. We indeed observe this type of linear relationship for Grp94, Hsp82, Hsp90α, HtpG, and Trap1 [Fig. 4(B,D); Supporting Information Figs. S3(B), S3(D), S3(F)]. We conclude that multiple Hsp90 family members can be inhibited by NECA and this inhibition is consistent with a simple competitive binding model.

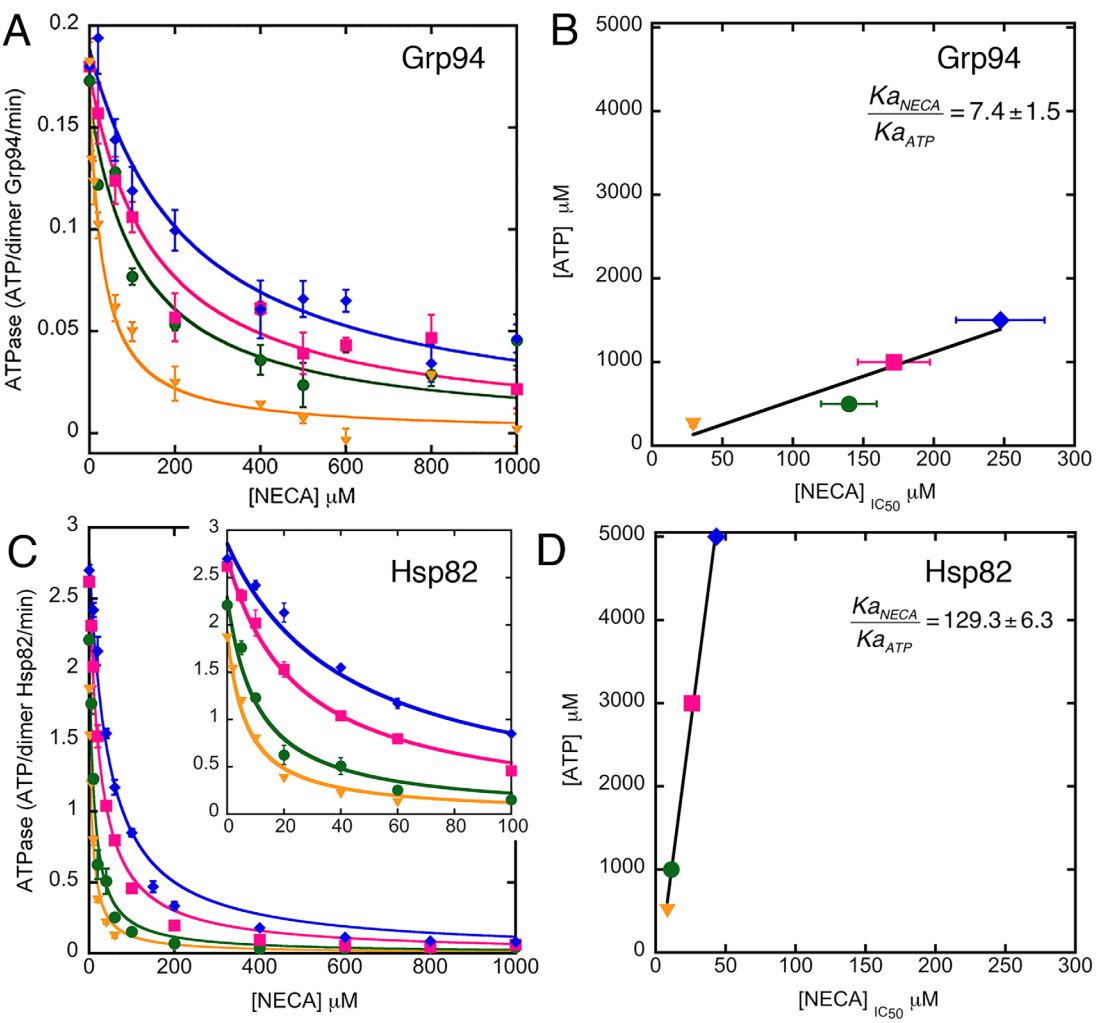

Figure 4. NECA has stronger inhibitory power for Hsp82 than Grp94. ATPase inhibition curves for Grp94 (**A**) and Hsp82 (**C**) were measured with variable background ATP concentrations. The solid lines are fits to Eq. (2). Error bars are the SEM for at least three measurements. ATP/$MgCl_2$ concentrations for Grp94: 250, 500, 1000, and 1500 μ*M*. ATP/$MgCl_2$ concentrations for Hsp82: 500, 1000, 3000, and 5000 μ*M*. (**B** and **D**) The NECA concentration at the inhibition midpoint, $[NECA]_{IC50}$, is linearly related to the background ATP concentration. Buffer conditions: 25 m*M* Tris pH 7.5, 150 m*M* KCl, 310 K.

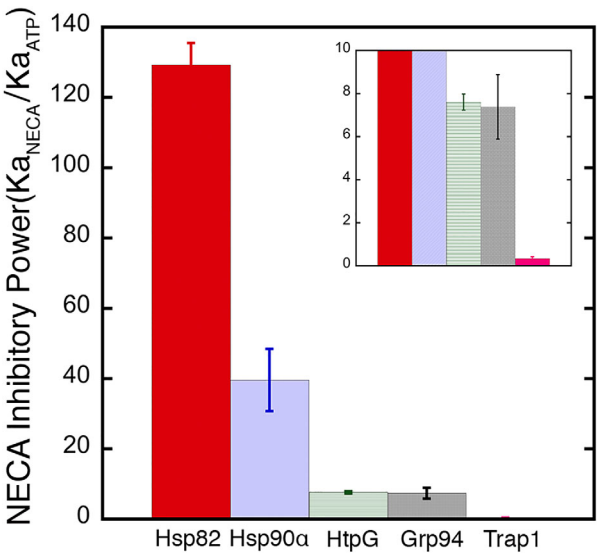

Figure 5. Ranking of inhibitory power of NECA for different Hsp90 family members.

The inhibitory power of NECA can be quantified by the degree to which NECA outcompetes ATP (K_a^{NECA}/K_a^{ATP}), where the readout of this competition is the reduction of ATPase activity. A simple competitive inhibition model directly equates K_a^{NECA}/K_a^{ATP} to the slope on plots of $[NECA]_{IC50}$ at different background concentrations of competing ATP [(Eq. (4) in "Methods"]. The large range of ATP concentrations in the competition experiments enables an accurate measurement of the slopes in Figure 4(B,D). It is visibly evident that NECA is a far stronger inhibitor of Hsp82 ($K_a^{NECA}/K_a^{ATP} = 129 \pm 6$) than Grp94 ($K_a^{NECA}/K_a^{ATP} = 7 \pm 2$).

We performed similar competition experiments on Hsp90α, HtpG, and Trap1 (Supporting Information Fig. S3). As shown in Figure 5, the resulting ranking of NECA inhibitory power (Hsp82 > Hsp90α > HtpG ≈ Grp94 > Trap1), places Grp94 as the second least sensitive to NECA inhibition. This ranking shows that NECA is not a Grp94-specific inhibitor.

Discussion

In this paper we show that NECA inhibits a wide variety of Hsp90 family members (Hsp82, Hsp90α, HtpG, Grp94, Trap1). The broad inhibition from NECA is not due to contaminating nucleotides or other compounds (Fig. 1). By measuring the capacity of NECA to outcompete the biologically relevant interactions with ATP we define an experimental scale of NECA's inhibitory power: Hsp82 > Hsp90α > HtpG ≈ Grp94 > Trap1. This scale ranks Grp94 as less sensitive to NECA inhibition (Fig. 5). Previous work suggested that cytosolic Hsp90 does not bind to NECA.[14] The cytosolic Hsp90 used in those experiments was derived from a native purification with minimal detected ATP binding and no measured ATPase activity. One explanation for the lack of NECA binding is that the Hsp90 structure and/or oligomeric state was compromised.

Our NMR assignment of the Grp94 NTD shows that NECA binding induces conformational changes that differ from ADP, consistent with a previously determined NECA-bound crystal structure (Fig. 2). The apo state of the Grp94 NTD appears to have high levels of conformational heterogeneity. We suggest that NECA binding reduces NTD conformational heterogeneity. Grp94 dynamics may be an important feature that could enable ligand-binding selectivity, as has been recently described for kinase inhibitors.[22]

Hsp82 shows the highest NECA sensitivity among the Hsp90s tested. We show direct binding to the Hsp82 NTD by NMR (Fig. 3). As expected for a nucleotide competitive inhibitor, NECA prevents closure of Hsp82 (Supporting Information Fig. S2). The structural origin for NECA's higher inhibitory power for Hsp82 is not clear. Our method for measuring NECA inhibitory power could be used to identify mutations on any Hsp90 as a way to test structural models of NECA specificity.

Our NECA inhibitory power measurements invoke a simple linkage model in which ATP and NECA compete for a single binding site. Because Hsp90 is a dimer, alternative cooperative models can be envisioned in which heterodimers with ATP and NECA bound on opposite arms have altered ATPase activities. Therefore, while our inhibitory power scale can appropriately rank Hsp90 proteins for their sensitivity to NECA, the K_a^{NECA}/K_a^{ATP} values themselves could change if a more complex linkage model is invoked.

NECA is an established adenosine receptor agonist.[23] Adenosine receptors are a family of G-coupled proteins that, upon stimulation from adenosine, activates adenylyl cyclase resulting in a cascade of biological outcomes.[24] Our results suggest that cell biological experiments utilizing NECA may have confounding effects from cytosolic Hsp90 inhibition.

Methods

The purifications of HtpG, mouse Grp94, human Hsp90α, human Trap1 and yeast Hsp82 have been described previously.[4,19,21] All full-length Hsp90 concentrations are reported per dimer. The Grp94 NTD (residues 72–287:GGGG:327-337) has the charged linker replaced by four glycine residues. The Grp94 NTD and the Hsp82 NTD (residues 1–210) were purified by immobilized Ni-affinity chromatography (Histrap HP, GE healthcare), TEV cleavage of the polyhistidine tag, subsequent Histrap removal of uncleaved material, followed by gel filtration (Superdex S-200, GE Healthcare). ^{15}N-labelled samples were expressed in an M9-medium containing $^{15}NH_4Cl$ (Cambridge Isotope Laboratories). $^{2}H/^{13}C/^{15}N$-labeled samples were expressed in an M9 medium containing

$^{15}NH_4Cl$, ^{13}C-glucose and 70% D_2O (Cambridge Isotope Laboratories).

HPLC-grade nucleotide samples were obtained from Sigma (ATP, AMP) and Acros (ADP, adenosine) and were all reported to be at least 98% pure by HPLC. NECA was purchased from Sigma and was reported to be at least 98% pure by TLC. Nucleotide samples were separated on a C18-AR reverse phase column (ACE) running at 0.3 mL/min at room temperature. ATP, ADP, and AMP were separated by a 9-min isocratic elution in 0.1*M* KH_2PO_4, pH 7.0. Adenosine and NECA were separated by a subsequent 21-min isocratic elution in 0.1*M* KH_2PO_4, pH 7.0, 20% methanol.

NMR experiments

NMR experiments (^1H–^{15}N TROSY-HSQC, HNCACB, HN(CO)CACB, ^{15}N-edited HSQC-NOESY) were performed on a Bruker Avance 800 MHz spectrometer. Backbone assignments of the Grp94-NTD were determined separately under apo conditions (600 μ*M* NTD) and saturating NECA (600 μ*M* NTD and 1.2 m*M* NECA). All experiments were processed in TopSpin (Bruker) and analyzed in ccpn (http://www.ccpn.ac.uk). NMR buffer conditions were 25 m*M* KH_2PO_4, pH 7.0, 50 m*M* KCl, 2 m*M* BME, 293 K.

Chemical shift perturbations of the Grp94 NTD were measured at saturating NECA concentration (150 μ*M* NTD and 300 μ*M* NECA) and saturating ADP (230 μ*M* NTD and 345 μ*M* ADP) with $MgCl_2$ concentration matching the ADP concentration. Chemical shift perturbations, Δδ, were calculated via

$$\Delta\delta = \left[(0.125 \times \Delta\delta_N)^2 + \Delta\delta_H^2 \right]^{\frac{1}{2}} \quad (1)$$

where $\Delta\delta_N$ and $\Delta\delta_H$ are the chemical shift changes in the nitrogen and proton dimensions, respectively.

ATPase measurements

ATPase activity of HtpG, Hsp82, Hsp90α, Trap1, and Grp94 was measured on a Microplate reader (BioTek) using a previously established enzyme linked assay.[25] Background absorption changes were measured prior to adding chaperone (Grp94/Hsp90α/Trap1: 0.75 μ*M*, HtpG/Hsp82:1.5 μ*M*). NECA had no influence on background measurements and no influence on the activity of the enzymes utilized in the assay. All measurements were performed at 310 K in 25 m*M* Tris, pH 7.5, 150 m*M* KCl with $MgCl_2$ concentration matched to the ATP concentration.

NECA inhibition curves were fit by nonlinear least squares (KaleidaGraph) to a simple competitive inhibition equation

$$\text{ATPase} = c \frac{K_a^{ATP}[ATP]}{1 + K_a^{ATP}[ATP]} \times \frac{1}{1 + K_{obs}[NECA]} \quad (2)$$

$$K_{obs} = \frac{K_a^{NECA}}{1 + K_a^{ATP}[ATP]} \quad (3)$$

where K_a^{NECA} and K_a^{ATP} are effective association constants, and the constant c scales the fraction of ATP bound to the ATPase activity. The observed equilibrium constant, K_{obs}, is the reciprocal of the inhibition curve midpoint, $[NECA]_{IC50}$. Therefore $[NECA]_{IC50}$ and the concentration of competing ATP are linearly related:

$$[ATP] = \frac{K_a^{NECA}}{K_a^{ATP}} \times [NECA]_{IC_{50}} - \frac{1}{K_a^{ATP}} \quad (4)$$

Standard error for $[NECA]_{IC50}$ values were determined for at least three separately-measured inhibition curves. Error bars for K_a^{NECA}/K_a^{ATP} values were determined by exhaustive enumeration of measured $[NECA]_{IC50}$ values that were then each fit to eq. (4). The standard error of the mean was determined from the resulting distribution of K_a^{NECA}/K_a^{ATP} values.

SAXS measurements

SAXS data was collected at the SIBYLS beamline.[26] Hsp82 (10 μ*M*) was incubated with AMPPNP and varying conditions of NECA. Samples were incubation in 25 m*M* Tris, pH 7.5, 150 m*M* KCl, 1 m*M* $MgCl_2$, 5 m*M* BME. SAXS data were analyzed with PRIMUS.[27]

Acknowledgments

We thank members of the Street lab for helpful discussions. Research for this project was supported by R01 GM115356.

References

1. Obermann WM, Sondermann H, Russo AA, Pavletich NP, Hartl FU (1998) *In vivo* function of Hsp90 is dependent on ATP binding and ATP hydrolysis. J Cell Biol 143:901–910.
2. Taipale M, Krykbaeva I, Koeva M, Kayatekin C, Westover KD, Karras GI, Lindquist S (2012) Quantitative analysis of HSP90-client interactions reveals principles of substrate recognition. Cell 150:987–1001.
3. Travers J, Sharp S, Workman P (2012) HSP90 inhibition: two-pronged exploitation of cancer dependencies. Drug Discov Today 17:242–252.
4. Southworth DR, Agard DA (2008) Species-dependent ensembles of conserved conformational states define the Hsp90 chaperone ATPase cycle. Mol Cell 32:631–640.
5. Ostrovsky O, Makarewich CA, Snapp EL, Argon Y (2009) An essential role for ATP binding and hydrolysis in the chaperone activity of GRP94 in cells. Proc Natl Acad Sci USA 106:11600–11605.
6. Leskovar A, Wegele H, Werbeck ND, Buchner J, Reinstein J (2008) The ATPase cycle of the mitochondrial Hsp90 analog Trap1. J Biol Chem 283:11677–11688.

7. Gewirth DT (2016) Paralog specific Hsp90 inhibitors—a brief history and a bright future. Curr Top Med Chem 16:2779–2791.
8. Marzec M, Eletto D, Argon Y (2012) GRP94: An HSP90-like protein specialized for protein folding and quality control in the endoplasmic reticulum. Biochim Biophys Acta 1823:774–787.
9. Chavany C, Mimnaugh E, Miller P, Bitton R, Nguyen P, Trepel J, Whitesell L, Schnur R, Moyer JD, Neckers L (1996) p185erbB2 binds to GRP94 *in vivo*. Dissociation of the p185erbB2/GRP94 heterocomplex by benzoquinone ansamycins precedes depletion of p185erbB2. J Biol Chem 271:4974–4977.
10. Mimnaugh EG, Chavany C, Neckers L (1996) Polyubiquitination and proteasomal degradation of the p185c-erbB-2 receptor protein-tyrosine kinase induced by geldanamycin. J Biol Chem 271:22796–22801.
11. Patel PD, Yan P, Seidler PM, Patel HJ, Sun W, Yang C, Que NS, Taldone T, Finotti P, Stephani RA, Gewirth DT, Chiosis G (2013) Paralog-selective Hsp90 inhibitors define tumor-specific regulation of HER2. Nat Chem Biol 9:677–684.
12. Xu W, Mimnaugh E, Rosser MF, Nicchitta C, Marcu M, Yarden Y, Neckers L (2001) Sensitivity of mature Erbb2 to geldanamycin is conferred by its kinase domain and is mediated by the chaperone protein Hsp90. J Biol Chem 276:3702–3708.
13. Xu W, Mimnaugh EG, Kim JS, Trepel JB, Neckers LM (2002) Hsp90, not Grp94, regulates the intracellular trafficking and stability of nascent ErbB2. Cell Stress Chaperones 7:91–96.
14. Rosser MF, Nicchitta CV (2000) Ligand interactions in the adenosine nucleotide-binding domain of the Hsp90 chaperone, GRP94. I. Evidence for allosteric regulation of ligand binding. J Biol Chem 275:22798–22805.
15. Soldano KL, Jivan A, Nicchitta CV, Gewirth DT (2003) Structure of the N-terminal domain of GRP94. Basis for ligand specificity and regulation. J Biol Chem 278: 48330–48338.
16. Patel HJ, Patel PD, Ochiana SO, Yan P, Sun W, Patel MR, Shah SK, Tramentozzi E, Brooks J, Bolaender A, Shrestha L, Stephani R, Finotti P, Leifer C, Li Z, Gewirth DT, Taldone T, Chiosis G (2015) Structure–activity relationship in a purine-scaffold compound series with selectivity for the endoplasmic reticulum Hsp90 paralog Grp94. J Med Chem 58:3922–3943.
17. Duerfeldt AS, Peterson LB, Maynard JC, Ng CL, Eletto D, Ostrovsky O, Shinogle HE, Moore DS, Argon Y, Nicchitta CV, Blagg BSJ (2012) Development of a Grp94 inhibitor. J Am Chem Soc 134:9796–9804.
18. Spooner RA, Hart PJ, Cook JP, Pietroni P, Rogon C, Höhfeld J, Roberts LM, Lord JM (2008) Cytosolic chaperones influence the fate of a toxin dislocated from the endoplasmic reticulum. Proc Natl Acad Sci USA 105: 17408–17413.
19. Krukenberg KA, Bottcher UM, Southworth DR, Agard DA (2009) Grp94, the endoplasmic reticulum Hsp90, has a similar solution conformation to cytosolic Hsp90 in the absence of nucleotide. Protein Sci 18:1815–1827.
20. Krukenberg KA, Forster F, Rice LM, Sali A, Agard DA (2008) Multiple conformations of E. coli Hsp90 in solution: insights into the conformational dynamics of Hsp90. Structure 16:755–765.
21. Cunningham CN, Krukenberg KA, Agard DA (2008) Intra- and intermonomer interactions are required to synergistically facilitate ATP hydrolysis in Hsp90. J Biol Chem 283:21170–21178.
22. Wilson C, Agafonov RV, Hoemberger M, Kutter S, Zorba A, Halpin J, Buosi V, Otten R, Waterman D, Theobald DL, Kern K (2015) Kinase dynamics. Using ancient protein kinases to unravel a modern cancer drug's mechanism. Science 347:882–886.
23. Schulte G, Fredholm BB (2000) Human adenosine A(1), A(2A), A(2B), and A(3) receptors expressed in Chinese hamster ovary cells all mediate the phosphorylation of extracellular-regulated kinase 1/2. Mol Pharmacol 58:477–482.
24. Jacobson KA, Gao ZG (2006) Adenosine receptors as therapeutic targets. Nat Rev Drug Discov 5:247–264.
25. Halpin JC, Huang B, Sun M, Street TO (2016) Crowding activates heat shock protein 90. J Biol Chem 291: 6447–6455.
26. Classen S, Hura GL, Holton JM, Rambo RP, Rodic I, McGuire PJ, Dyer K, Hammel M, Meigs G, Frankel KA, Tainer JA (2013) Implementation and performance of SIBYLS: a dual endstation small-angle X-ray scattering and macromolecular crystallography beamline at the advanced light source. J Appl Crystallogr 46:1–13.
27. Petoukhov MV, Franke D, Shkumatov AV, Tria G, Kikhney AG, Gajda M, Gorba C, Mertens HDT, Konarev PV, Svergun DI (2012) New developments in the program package for small-angle scattering data analysis. J Appl Crystallogr 45:342–350.